BIOCHEMISTRY
including biophysical chemistry & molecular biology
Article

Biochemistry **2010,** *49,* 2097–2109 2097
DOI: 10.1021/bi901977k

Investigation of Translocation, DNA Unwinding, and Protein Displacement by NS3h, the Helicase Domain from the Hepatitis C Virus Helicase†

Dennis L. Matlock,[§,@] Laxmi Yeruva,[‡,@] Alicia K. Byrd,[‡] Samuel G. Mackintosh,[‡] Clint Langston,[§] Carrie Brown,[§] Craig E. Cameron,[∥] Christopher J. Fischer,*[,⊥] and Kevin D. Raney*[,‡]

[‡]*Department of Biochemistry and Molecular Biology, University of Arkansas for Medical Sciences, Little Rock, Arkansas 72205,* [§]*Department of Chemistry, Harding University, Searcy, Arkansas 72143,* [∥]*Department of Biochemistry and Molecular Biology, The Pennsylvania State University, University Park, Pennsylvania 16802, and* [⊥]*Department of Physics and Astronomy, University of Kansas, Lawrence, Kansas 66045* [@]*These authors contributed equally to this work.*

Received November 16, 2009; Revised Manuscript Received January 14, 2010

ABSTRACT: Helicases are motor proteins that are involved in DNA and RNA metabolism, replication, recombination, transcription, and repair. The motors are powered by ATP binding and hydrolysis. Hepatitis C virus encodes a helicase called nonstructural protein (NS3). NS3 possesses protease and helicase activities on its N-terminal and C-terminal domains, respectively. The helicase domain of NS3 is termed NS3h. In vitro, NS3h catalyzes RNA and DNA unwinding in a 3′−5′ direction. The directionality of unwinding is thought to arise in part from the enzyme's ability to translocate along DNA, but translocation has not been shown explicitly. We examined the DNA translocase activity of NS3h by using single-stranded oligonucleotide substrates containing a fluorescent probe on the 5′ end. NS3h can bind to the ssDNA and in the presence of ATP move toward the 5′ end. When the enzyme encounters the fluorescent probe, a fluorescence change is observed that allows translocation to be characterized. Under conditions that favor binding of one NS3h per DNA substrate (100 nM NS3h and 200 nM oligonucleotide), we find that NS3h translocates on ssDNA at a rate of 46 ± 5 nucleotides/s, and that it can move for 230 ± 60 nucleotides before dissociating from the DNA. The translocase activity of some helicases is responsible for displacing proteins that are bound to DNA. We studied protein displacement by using a ssDNA oligonucleotide covalently linked to biotin on the 5′ end. Upon addition of streptavidin, a "protein block" was placed in the pathway of the helicase. Interestingly, NS3h was unable to displace streptavidin from the end of the oligonucleotide, despite its ability to translocate along the DNA. The DNA unwinding activity of NS3h was examined using a 22 bp duplex DNA substrate under conditions that were identical to those used to study translocation. NS3h exhibited little or no DNA unwinding under single-cycle conditions, supporting the conclusion that NS3h is a relatively poor helicase in its monomeric form, as has been reported. In summary, NS3h translocates on ssDNA as a monomer, but the translocase activity does not correspond to comparable DNA unwinding activity or protein displacement activity under identical conditions.

Helicases are nucleic acid-dependent ATPases that are involved in several processes such as DNA replication, repair, transcription, translation, RNA maturation, splicing, and nuclear export processes (*1*−*4*). Helicases have been divided into different superfamilies such as SF1−SF4 on the basis of sequence analysis (*5*). The functional forms of helicases include oligomers (such as hexamers, trimers, or dimers) and monomers (*6*−*10*). In vitro, DNA helicases translocate along single-stranded DNA in a reaction that is coupled to ATP binding and hydrolysis. Upon encountering duplex DNA, DNA can unwind; however, the specific relationship between translocation and DNA unwinding has not been made clear for most helicases. Helicases that unwind DNA can displace proteins from nucleic acids while translocating along the DNA (*11*−*14*). Mutations in helicase genes lead to genomic instability which results in diseases such as Blooms syndrome, Werner syndrome, and cancer (*15*).

A fundamental question regarding helicase activity is the degree to which DNA unwinding is coupled to translocation activity (*16*). For example, DNA unwinding might be a consequence of translocation. In such a mechanism, DNA unwinding occurs due to strong interaction with one of the strands of the duplex (the translocase or bound strand) and steric displacement of the complementary strand (displaced strand) (*17*−*19*). Alternatively, specific protein−nucleic acid interactions might result in DNA melting so that DNA unwinding might be uncoupled from translocase activity (*20*). Dillingham et al. developed a fluorescence stopped-flow assay to study translocation on single-stranded DNA (ssDNA) by the *Bacillus stearothermophilus* PcrA helicase (*21*). Later this method was modified and used by Fischer et al. to characterize the kinetic mechanism of UvrD translocation along ssDNA using global nonlinear least-squares (NLLS) analysis of the kinetic time courses (*22*−*26*). These studies demonstrated that *Escherichia coli* UvrD and Rep translocate progressively in the 3′−5′ direction on ssDNA (*23*, *26*). However, there is not a direct relationship between translocase activity and DNA unwinding for UvrD and Rep helicases. Under single-cycle conditions with respect to the DNA substrate, an oligomeric form of UvrD helicase unwinds double-stranded DNA (dsDNA) whereas a monomer is capable of translocating along ssDNA (*22*).

†This work was supported by NIH research grants R24 GM080599 (K.D.R.), R01 GM089001 (K.D.R. and C.E.C.), and NIH Grant # P20 RR-16460 from the IDeA Networks of Biomedical Research Excellence (INBRE) Program of the National Center for Research Resources.

*To whom correspondence should be addressed. K.D.R.: telephone, (501) 685-5244; fax, (501) 686-8169; e-mail, raneykevind@uams.edu. C.J.F.: telephone, (785) 864-4579; fax, (785) 864-5262; e-mail, shark@ku.edu.

Published on Web 01/28/2010

The monomeric form of UvrD does not produce ssDNA under single-cycle conditions (*22*). Similar results have been reported for PcrA (*25*) and Rep (*26*) helicases based on global NLLS analysis, indicating that oligomerization strongly stimulates DNA unwinding activity but is not required for translocase activity. However, a truncated form of Rep does unwind dsDNA as a monomer, and interactions between PcrA and Rep with other DNA binding proteins strongly stimulate the DNA unwinding activity in vitro (*26*). Therefore, the relationship between DNA unwinding and translocase activity can vary depending on the mechanism of the particular helicase, the form of the helicase, and the presence or absence of appropriate binding partners.

An activity associated with helicase translocation is the removal of proteins from DNA as a result of movement of the enzyme along the DNA (*11*−*14*). For example, PcrA and UvrD can displace RecA protein filaments from ssDNA (*27*, *28*). A method for measuring protein displacement has been developed in which biotin-labeled oligonucleotides are labeled with streptavidin to create protein blocks on the end of the DNA. Displacement of streptavidin can be measured as a result of directionally biased movement of a helicase on ssDNA (*12*, *13*).

Hepatitis C virus (HCV) nonstructural protein 3 (NS3) is a SF2 helicase (*29*). The 180 N-terminal amino acids constitute a serine protease, and the 450 C-terminal amino acids make up the helicase (*30*). NS3 catalyzes RNA and DNA unwinding in a 3′−5′ direction as judged by the need for a 3′ single-stranded overhang attached to the duplex (*29*, *30*). Displacement of streptavidin from the 3′ end of biotin-labeled oligonucleotides by NS3 also supports the 3′−5′ directionality on ssDNA (*14*).

Full-length NS3 is capable of interacting with itself in vitro. Tackett et al. have reported that multiple NS3 molecules binding to the single-stranded region of a partial duplex DNA substrate were required for optimal DNA unwinding activity in vitro (*31*). Sikora et al. demonstrated optimal DNA unwinding activity by an oligomeric species of NS3 based on DNA unwinding, chemical cross-linking, and biophysical approaches (*32*). Serebrov and Pyle reported that NS3 unwinds RNA as a dimer with an 18 bp kinetic step size (*33*). The helicase domain of NS3 is termed NS3h; however, it does not readily interact with itself, based on biochemical and biophysical studies (*32*).

The mechano-chemical mechanism(s) of helicase stepping and coupling of ATP hydrolysis to DNA or RNA unwinding has received much attention (*10*, *16*, *21*, *23*, *33*, *34*). Dumont et al. reported NS3 functions as a monomer in optical trap experiments with an 11 bp step size which consisted of smaller physical steps of 2−3 bp (*35*). Single-molecule fluorescence energy transfer measurements supported a "spring-loaded" mechanism for NS3, whereby two or three small steps of one nucleotide are taken which builds up tension in the molecule leading to simultaneous unwinding of 2−3 bp (*36*). Levin et al. have studied NS3h binding and unwinding of DNA and concluded that the enzyme functions as a Brownian motor in which binding of ATP causes the enzyme to enter a loosely bound state in which the helicase is free to diffuse forward or backward by Brownian motion (*37*). Interaction with the ssDNA−dsDNA junction facilitates ATP hydrolysis, resulting in a forward "power stroke" for the proposed Brownian motor.

Optimal DNA unwinding by NS3 and NS3h requires that multiple molecules of enzyme be bound to the substrate (*31*, *32*, *38*). However, recent work indicates that a single-stranded binding (SSB) protein can substitute, at least to some degree, for the need for multiple helicase molecules because monomeric NS3h was found to be able to unwind DNA when coupled with an SSB (*39*). Hence, DNA unwinding and RNA unwinding by NS3 and NS3h have received much attention, and their respective mechanisms are of interest as model systems as well as in relation to hepatitis C viral replication. In contrast to DNA and RNA unwinding, translocation of NS3 or NS3h on a single-stranded nucleic acid has not been directly demonstrated.

In this report, the fluorescence stopped-flow assay using labeled oligonucleotides and global NLLS analysis was used to study translocation on ssDNA by the hepatitis C virus NS3 helicase domain. Experiments were performed under single-cycle conditions that favor binding of monomeric NS3h to the DNA substrate to determine the rate constants, kinetic step size, directionality, and processivity of NS3h using global NLLS analysis. DNA unwinding and streptavidin displacement were also investigated under identical conditions to compare the different activities associated with NS3h.

EXPERIMENTAL PROCEDURES

Materials. ATP (disodium salt), streptavidin, phosphoenolpyruvate (tricyclohexylammonium salt), pyruvate kinase/lactate dehydrogenase (in glycerol), heparin (sodium salt), poly(dT), sodium dodecyl sulfate (SDS), potassium acetate, magnesium acetate, bromophenol blue, and xylene cyanol were obtained from Sigma. [γ-^{32}p]ATP was obtained from Perkin-Elmer Life Sciences. DNA oligonucleotides were purchased from Integrated DNA Technologies, purified by denaturing polyacrylamide gel electrophoresis, and stored in 10 mM Hepes (pH 7.5) and 1 mM EDTA. Purified oligonucleotides were quantified by UV absorbance at 260 nm in 0.2 M KOH by using extinction coefficients. Recombinant full-length NS3 was derived from the HCV Con 1B replicon consensus sequence and purified as described previously (*31*). NS3h was also derived from the HCV Con 1B replicon consensus sequence and purified as described previously (*40*).

Heparin was dialyzed against Milli-Q water using 3500 Da molecular mass cutoff dialysis tubing. The heparin stock solution concentration was determined by barbital buffer and titration with Azure A using previously published protocols (*21*−*25*).

Assay buffer contains 25 mM MOPS (pH 7.0), 50 mM NaCl, 0.1 mM EDTA, 2 mM β-mercaptoethanol (BME), and 0.1 mg/mL bovine serum albumin (BSA). For dissociation experiments, the same assay buffer was prepared without BSA.

DNA Unwinding. The substrate used to monitor NS3 and NS3h unwinding was prepared by annealing a 37-mer with a 22-mer resulting in a 37-mer·22-mer partial duplex containing a T15 single-stranded overhang and 22 bp. The sequence of the loading strand was 3′-TTTTTTTTTTTTTTTAGGACAGTC-GGATCGCAGTCAG-5′ (also termed translocase or bound strand in some reports), and the displaced strand was 5′-TCCTG-TCAGCCTAGCGTCAGTC-3′. The trapping strand was complementary to the 22-mer displaced strand (5′-GACTGACGC-TAGGCTGACAGGA-3′). Oligonucleotides were purified by preparative gel electrophoresis. Crude oligonucleotide was mixed with 90% formamide (1:1) and resolved on a 7 M urea−20% polyacrylamide gel (Hoeffer Scientific instruments). Oligonucleotide was excised from the gel by visualization under UV followed by electroelution of the sliced gel using a Schleicher and Schull elutrap apparatus. Oligonucleotides were then desalted on a Waters Sep-Pak C_{18} column and lyophilized overnight using a Savant Speed-Vac. Lyophilized oligonucleotides were suspended in 10 mM Hepes (pH 7.5) and 1 mM EDTA, and the concentration

was determined by measuring the absorbance at 260 nm in 0.2 M KOH using calculated extinction coefficients. To prepare a partial duplex substrate, a 1:2 mixture of 37-mer to 22-mer was mixed, heated at 95 °C for 10 min, and allowed to cool to room temperature. The mixture of partial duplex was resolved on a native 20% acrylamide gel, electroeluted, desalted, and quantified as described above.

The purified 37-mer·22-mer partial duplex was radiolabeled at the 5′ end with [γ-^{32}P]ATP by T4 polynucleotide kinase. The substrate was incubated for 1 h at 37 °C, followed by heat denaturation of the enzyme at 70 °C for 10 min. Then unlabeled complementary oligonucleotide to 22-mer was added to the 5′-radiolabeled substrate. Excess [γ-^{32}P]ATP was removed when the substrate was passed through two 1 mL Sephadex G-25 sping columns. The mixture (5′-radiolabeled and unlabeled complementary oligonucleotide) was heated to 95 °C and slowly cooled to room temperature. To prepare higher substrate concentrations, unlabeled partial duplex DNA was added to radiolabeled substrate, heated to 95 °C, and slowly cooled to room temperature.

DNA unwinding experiments were conducted using a KinTek rapid chemical quench-flow instrument maintained at 37 °C with a circulating water bath. All concentrations listed are final concentrations after mixing. Unwinding assay buffer contained 25 mM MOPS (pH 7.0), 50 mM NaCl, 0.1 mM EDTA, 2 mM BME, and 0.1 mg/mL BSA. All unwinding experiments were conducted under single-cycle conditions with respect to the DNA substrate by including heparin as a protein trap. For experiments in the presence of excess enzyme over DNA substrate, a "two-step" mixing procedure was applied. DNA (37-mer·22-mer, 2 nM) was incubated with NS3 or NS3h (500 nM) for 20 s prior to initiation of unwinding by addition of 5 mM ATP and 10 mM $MgCl_2$. The DNA annealing trap (60 nM) and heparin (4 mg/mL) were added along with ATP and $MgCl_2$ to prevent protein rebinding to the DNA and to prevent reannealing of the ssDNA products. After the solution had been rapidly mixed, the reaction was quenched with 200 mM EDTA and 0.7% SDS. A 25 μL aliquot of quenched reaction mixture was added to 5 μL of loading buffer (30% glycerol, 0.1% bromophenol blue, and 0.1% xylene cyanol), and products were electrophoresed on a 20% acrylamide gel at 22 mA for 2.5 h. The gel was exposed to a phosphor storage screen, and the quantity of ssDNA and dsDNA was determined by using ImageQuant. To determine the efficiency of heparin as a protein trap, DNA substrate (2 nM) and heparin (4 mg/mL) were incubated together prior to rapid addition of NS3h (500 nM). After 20 s, the unwinding reaction was initiated by addition of ATP (5 mM), $MgCl_2$ (10 mM), and annealing trap (60 nM). For experiments conducted under conditions of excess substrate concentration relative to enzyme concentration, DNA (37-mer·22-mer, 200 nM) was incubated with NS3 or NS3h (100 nM) prior to initiation of unwinding with 5 mM ATP and 10 mM $MgCl_2$, 4 mg/mL heparin, and the DNA annealing trap (2 μM). To determine the efficiency of heparin as a protein trap under conditions of excess substrate concentration, DNA substrate (37-mer·22-mer, 200 nM) was incubated with 4 mg/mL heparin, 5 mM ATP, 10 mM $MgCl_2$, and 2 μM DNA annealing trap prior to initiation of DNA unwinding by addition of NS3h (100 nM). The reaction was quenched; loading dye was added, and products were separated by electrophoresis and quantitated as described above.

Streptavidin Displacement. This assay was performed by using two 5′-biotinylated oligonucleotides in which biotin label (Biotin dT) was incorporated into the DNA. The sequence of the 5′-bio-30-mer (29 nucleotides with Biotin dT) was 5′-G**X**$(T)_{28}$-3′, and the sequence of the 5′-bio-60-mer (59 nucleotides with Biotin dT) was 5′-G**X**$(T)_{58}$-3′, where **X** indicates placement of the biotin label in the DNA sequence. Streptavidin (50 μM) was prepared in buffer containing 25 mM Hepes (pH 7.5), 20% glycerol, and 10 mM NaCl. The solution was quick-frozen in liquid nitrogen and stored at −80 °C. Prior to use, streptavidin was diluted to 5 μM in buffer consisting of 25 mM Hepes (pH 7.5), 0.1 mg/mL BSA, 0.1 mM EDTA, and 1 mM BME. Oligonucleotide (10 or 200 nM) was incubated in reaction buffer [25 mM MOPS (pH 7.0), 12.5 mM $Mg(OAc)_2$, 150 mM KOAc, 4 mM PEP, 1 mM BME, and 0.1 mg/mL BSA] with 5 mM ATP, 300 nM streptavidin, and PK and LDH (10.8 and 16.6 units/mL, respectively) at 37 °C for 3 min. For experiments that utilized 200 nM oligonucleotide, 6 μM streptavidin was included rather than 300 nM streptavidin, to maintain the same ratio of DNA to streptavidin in all the experiments. The streptavidin displacement reaction was initiated by addition of helicase. At various times, 10 μL aliquots were removed from the reaction mixture and mixed with 10 μL of quench solution [0.6% SDS, 200 mM EDTA (pH 8.0), 10 μM poly(dT), 0.08% xylene cyanol, 0.08% bromophenol blue, and 10% glycerol]. Samples were analyzed by electrophoresis on a 15% polyacrylamide gel. Radiolabeled DNA bands were visualized by using a phosphorimager, and the quantity of radioactivity in the bands corresponding to free oligonucleotide and streptavidin-bound oligonucleotide in each sample was determined by using ImageQuant. The fraction of free oligonucleotide in samples was calculated with a correction for the free oligonucleotide in the blank sample by using the following equation.

$$FD_{c,t} = \frac{\dfrac{FD_t}{FD_t + SD_t} - \dfrac{FD_b}{FD_b + SD_b}}{1 - \dfrac{FD_b}{FD_b + SD_b}}$$

$FD_{c,t}$ is the fraction of free oligonucleotide corrected for the amount of free oligonucleotide in the blank sample, FD_t is the radioactivity of free oligonucleotide DNA for each sample at time t, SD_t is the radioactivity of streptavidin-bound oligonucleotide DNA at time t, and FD_b and SD_b are the radioactivities of free oligonucleotide DNA and streptavidin-bound oligonucleotide DNA, respectively, in the blank (b) at time zero.

Dissociation of NS3h from ssDNA. Dissociation experiments were performed as described previously (*22*, *25*). Briefly, dissociation kinetics were determined by an increase in NS3h tryptophan fluorescence (λ_{ex} = 280 nm, and λ_{em} = 345 nm). The dissociation rate constant (k_d) was measured during NS3h translocation on ssDNA [poly(dT)].

Translocation of NS3h on ssDNA. Translocation experiments were performed in assay buffer [25 mM MOPS (pH 7.0), 50 mM NaCl, 0.1 mM EDTA, 1 mM β-mercaptoethanol, and 0.1 mg/mL bovine serum albumin] at 37 °C using an SX18MV stopped-flow instrument (Applied Photophysics Ltd., Surrey, U.K.). During translocation experiments, 100 nM NS3h was preincubated with 200 nM ssDNA and the reaction was initiated by the addition of 5 mM ATP, 10 mM $MgCl_2$, and 4 mg/mL heparin. These are final concentrations after mixing in the stopped-flow instrument. NS3h translocation was assessed as described previously (*22*). Briefly, fluorescence change was measured upon arrival of NS3h at the 5′ end of ssDNA using 5′-F-$(dT)_L$ (λ_{ex} = 492 nm, and λ_{em} > 520 nm).

Scheme 1

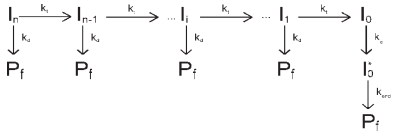

Scheme 2

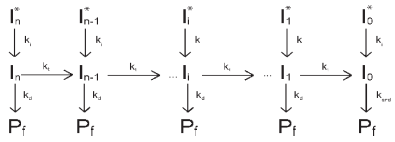

Analysis of Kinetic Translocation Data. The multiple time courses for NS3h monomer translocation on DNA, each corresponding to a different length of DNA, were analyzed globally using eq 1 (derived from Scheme 1) or eq 2 (derived from Scheme 2) and standard nonlinear least-squares (NLLS) algorithms to obtain estimates of the translocation kinetic parameters (*22*−*26*). In these equations, the variables k_t, k_d, k_c, k_i, k_{end}, m, d, B, C, r, and rn were constrained to be global parameters (independent of DNA length); the A variables were allowed to float for each time course (*23*−*26*). The multiple time courses for NS3h monomer translocation on poly(dT), each corresponding to a different solution concentration of heparin, were analyzed separately using eq 3. All NLLS and linear least-squares analyses were performed using Conlin (*41*), kindly provided by J. Williams. The software library CNL50 (Visual Numerics Inc., Houston, TX) was used for the numerical calculation of the inverse Laplace transform.

RESULTS

DNA Unwinding with the Enzyme Concentration in Excess of the Substrate Concentration. To investigate the relationship between translocation on ssDNA and unwinding of dsDNA for NS3h and for NS3, we sought conditions that could be applied to each type of measurement and to each form of the enzyme. NS3 exhibits a large kinetic step size as well as relatively low processivity. A DNA substrate was prepared that would be short enough to exhibit a single kinetic step (and therefore more product) but was stable enough to use at 37 °C. The substrate contained 15 nucleotides of a ssDNA overhang and 22 bp (37nt:22bp). To evaluate the substrate, we performed standard DNA unwinding experiments in which the helicase concentration exceeded the DNA substrate concentration. Typical experiments for measuring DNA unwinding by a helicase are conducted by incubating the helicase with the DNA substrate, followed by rapid mixing with ATP and Mg^{2+} to initiate the reaction. However, we found that this protocol does not work well with NS3h when the helicase concentration is in excess of the DNA substrate concentration due to ATP-independent DNA unwinding (*42*).

DNA unwinding by NS3h has been studied extensively by using a "double-mixing" approach as described by Levin et al. (*38*). We applied this approach to compare DNA unwinding by NS3h and NS3 under identical conditions (Figure 1). Helicase is rapidly mixed with DNA substrate and allowed to incubate for 20 s, which is too little time for ATP-independent melting to occur. After the 20 s incubation time, ATP and Mg^{2+} are introduced in a second rapid mixing step, followed by varying reaction times before the reaction is stopped with quencher. Using this approach, we were able to directly compare DNA unwinding by NS3 and NS3h under identical conditions. NS3 or NS3h (500 nM) was rapidly mixed with DNA (2 nM) followed by a second rapid mixing step in which ATP and $MgCl_2$ were added. To prevent reannealing of ssDNA products, a 22-mer DNA annealing trap

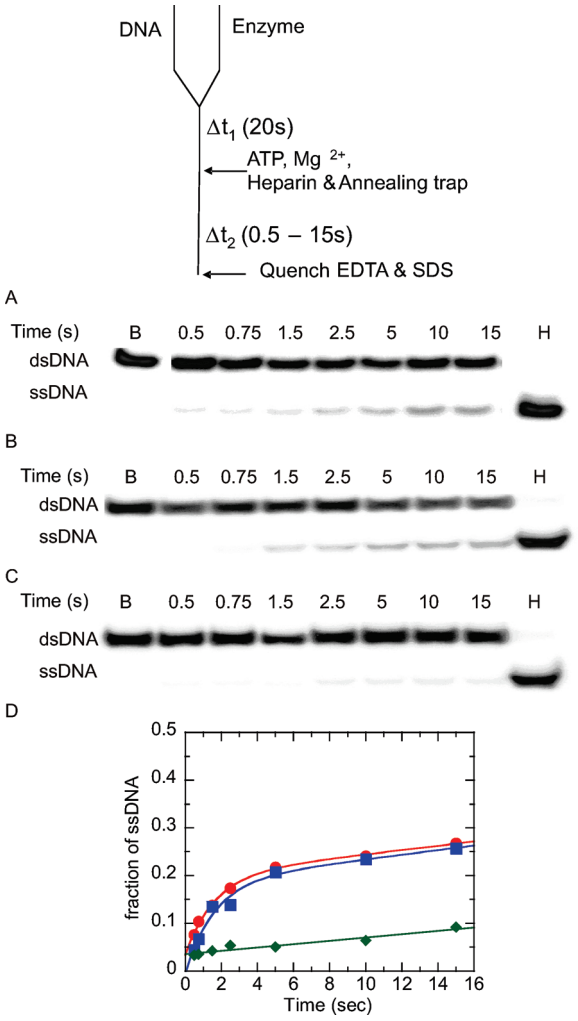

FIGURE 1: Unwinding of the 37-mer·22-mer partial duplex by NS3 and NS3h in the presence of heparin (used as a protein trap) with the enzyme concentration in excess of the DNA substrate concentration. A "double-mixing" experimental protocol was performed as described in the text. Unwinding products were resolved on a 20% polyacrylamide gel, visualized using a PhosphorImager, and quantitated by using ImageQuant. (A) Representative gel image showing unwinding of 2 nM partial duplex by 500 nM NS3. The blank sample (B) shows the partial duplex DNA substrate prior to unwinding, and the heated sample (H) shows the DNA after it has been heated to 95 °C for 10 min. (B) Representative gel image showing unwinding of 2 nM partial duplex by 500 nM NS3h. (C) To determine the efficiency of heparin as a protein trap, we mixed the partial duplex substrate (2 nM) with heparin (4 mg/mL) prior to initiating the reaction upon mixing with NS3h (500 nM). Little or no unwinding was observed. (D) Fraction of product formation for unwinding of 2 nM partial duplex by 500 nM NS3 (circles), 500 nM NS3h (squares), and 500 nM NS3h under conditions where heparin and partial duplex DNA were mixed together prior to initiation of the reaction by addition of enzyme. Enzyme-catalyzed unwinding was fit to a single exponential followed by a steady state rate, resulting in amplitudes of 0.19 ± 0.03 and 0.17 ± 0.01 nM, rate constants of 0.62 ± 0.3 and 0.61 ± 0.1 s^{-1}, and steady state rates of 0.005 ± 0.001 and 0.004 ± 0.001 nM/s for NS3 and NS3h, respectively. The control experiment in which heparin was added to the DNA substrate prior to addition of NS3h was fit to a linear equation, resulting in a rate of 0.004 ± 0.001 nM/s (diamonds).

was included with the ATP and $MgCl_2$, which was complementary to the 22-mer of the 37-mer·22-mer DNA substrate. To maintain single-cycle conditions, heparin was also added to "trap" protein that dissociated from the DNA substrate. The efficiency of heparin as a protein trap was tested via addition of heparin to the DNA substrate prior to the first mixing step. Under these conditions, a small amount of DNA unwinding was observed, which indicated heparin as a good but not perfect protein trap under these conditions (Figure 1C). NS3 and NS3h unwind DNA almost identically, producing ~20% ssDNA product when incubated with substrate for only 20 s prior to initiation of the unwinding reaction (Figure 1D). In contrast, NS3 unwinds nearly 80% of a 30 bp DNA substrate when incubated for at least 10 min prior to initiation of the reaction (*29*−*31*, *40*). Therefore, the incubation time between NS3 and DNA can affect the level of DNA unwinding, which has been reported for NS3 unwinding of RNA (*43*). The slow phase for DNA unwinding following the initial burst of product formation is likely due to slight leakage of the protein trap based on similar rates for the slow phase compared to the control experiment (Figure 1D).

DNA Unwinding with the DNA Substrate Concentration in Excess of the Enzyme Concentration. Translocation on ssDNA has been best studied under conditions that favor binding of one molecule of helicase per one molecule of substrate (*16*). To achieve these conditions, the concentration of oligonucleotide substrate must be in excess of the helicase concentration. DNA unwinding experiments were conducted under these conditions, in which the DNA substrate concentration (200 nM) exceeded the enzyme concentration (100 nM). NS3h has been shown to exist as a monomer in the presence and absence of ssDNA (*32*, *44*) (Figure 1 of the Supporting Information). When NS3h is preincubated with the DNA substrate under these conditions, no ATP-independent unwinding was observed (K. A. Reynolds and K. D. Raney, manuscript in preparation). Therefore, only one mixing step was necessary for unwinding experiments to be performed. NS3 or NS3h (100 nM) and DNA (200 nM) were incubated prior to initiation of unwinding by addition of ATP, $MgCl_2$, heparin, and annealing trap (Figure 2). Under single-cycle conditions, little or no unwinding was observed (Figure 2A, B,D). The efficiency of the heparin as a protein trap was tested under these conditions by incubating DNA with ATP, $MgCl_2$, heparin, and annealing trap prior to initiation of unwinding with NS3h which led to no observable unwinding over background, indicating that heparin functions as an excellent protein trap under these conditions (Figure 2C,D).

Protein Displacement by NS3 and NS3h. Helicase activities are not limited to melting duplex DNA. Helicases can also displace proteins from DNA during DNA unwinding. Displacement of streptavidin from biotin-labeled oligonucleotides has been used to measure protein displacement activity on ssDNA. A 5′-bio-29-mer and a 5′-bio-59-mer were examined for the comparison of the protein displacement activities of NS3 and NS3h on ssDNA. The reaction was initiated by the addition of NS3 or NS3h to the biotin-labeled DNA substrate (10 nM) in the presence of ATP, Mg^{2+}, and excess biotin which served to trap streptavidin. Aliquots were removed and quenched at various times, followed by native polyacrylamide gel electrophoresis to separate free oligonucleotide from streptavidin-bound oligonucleotide (Figures 3 and 4). The magnitude of the gel band due to streptavidin-bound oligonucleotide decreased during the 60 min incubation with NS3 for the 5′-bio-29-mer and 5′-bio-59-mer,

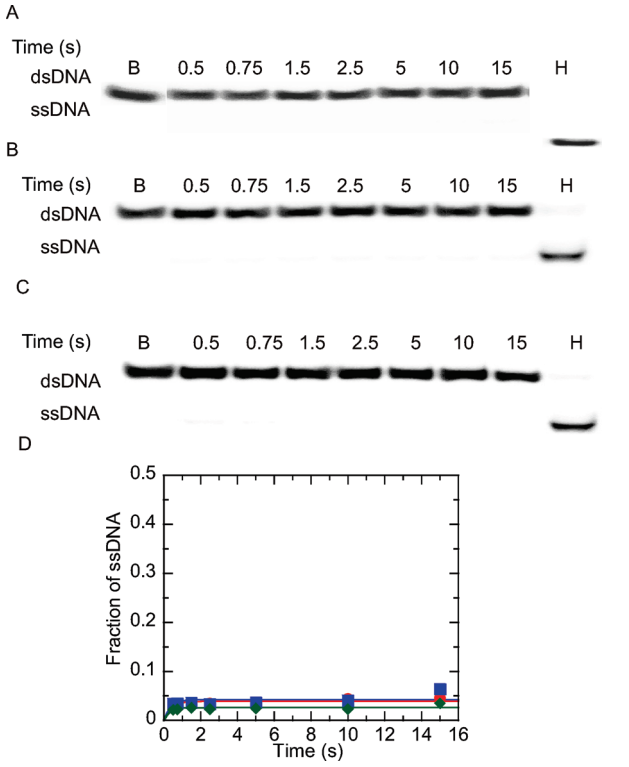

FIGURE 2: Unwinding of the 37-mer·22-mer partial duplex by NS3 and NS3h with the DNA substrate concentration in excess of the enzyme concentration. Unwinding products were resolved by electrophoresis on a 20% native polyacrylamide gel, visualized using a PhosphorImager, and quantitated by using ImageQuant. (A) Representative gel image showing unwinding of 200 nM partial duplex DNA by 100 nM NS3. The blank sample (B) shows the DNA substrate prior to unwinding, and the heated sample (H) shows the substrate after being heated to 95 °C. (B) Representative gel image showing unwinding of 200 nM partial duplex DNA by 100 nM NS3h. (C) Heparin (4 mg/mL) was mixed with the partial duplex substrate (200 nM) prior to initiation of the reaction by mixing with NS3h (100 nM) to determine the ability of heparin to serve as a protein trap. (D) Fraction of ssDNA product formed after quantitation of gel images by using ImageQuant. Unwinding of 200 nM 37-mer·22-mer DNA by 100 nM NS3 (circles), 100 nM NS3h (squares), and 500 nM NS3h under conditions where heparin and partial duplex DNA were mixed together prior to initiation of the reaction by addition of enzyme (diamonds).

indicating the displacement of streptavidin from biotin-labeled oligonucleotide (Figure 3A,B). Similarly, the streptavidin displacement reaction was also performed by the addition of 1 μM NS3h to 10 nM substrate; however, no streptavidin displacement was observed in the presence of NS3h (Figure 4A,B).

To mimic the conditions used for translocation assays (described below), we conducted streptavidin displacement experiments by adding 100 nM NS3h to 200 nM substrate prior to the reaction. No product was observed with either substrate (5′-bio-29-mer or 5′-bio-59-mer) during the 60 min incubation, which indicated no streptavidin displacement under these conditions (Figures 3C,D and 4C,D). In summary, NS3 was capable of displacing streptavidin from both DNA substrates under conditions in which the helicase concentration greatly exceeded the substrate concentration. However, when the NS3 concentration (100 nM) was less than the substrate concentration (200 nM), no streptavidin displacement was observed during the 60 min incubation (Figure 3). NS3h was unable to displace streptavidin from either biotin-labeled oligonucleotide, regardless of the relative concentrations of enzyme and substrate (Figure 4). Hence, the DNA

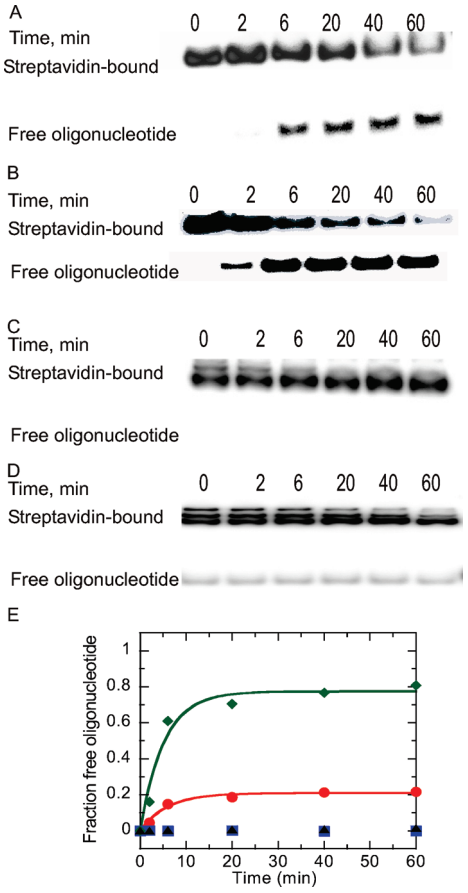

FIGURE 3: NS3-catalyzed streptavidin displacement from 5′-bio-30-mer and 5′-bio-60-mer oligonucleotides. (A) NS3 (1 μM) was incubated with 5′-bio-30-mer (10 nM) in reaction buffer. Samples were removed at varying times and added to a quencher solution (0.6% SDS, 200 mM EDTA, 0.08% xylene cyanol, 0.08% bromophenol blue, and 10% glycerol) followed by separation of streptavidin-bound oligonucleotide from free oligonucleotide on a 15% native polyacrylamide gel. (B) NS3 (1 μM) was incubated with 10 nM 5′-bio-60-mer in reaction buffer and treated as described for panel A. (C) NS3 (100 nM) was incubated with 200 nM 5′-bio-30-mer under identical conditions as described for panel A, and samples were analyzed by 15% native polyacrylamide gel electrophoresis. (D) NS3 (100 nM) was incubated with 200 nM 5′-bio-60-mer under identical conditions as described for panel A. (E) Displacement of streptavidin from different lengths of biotin oligonucleotides catalyzed by NS3. Results were obtained by quantitation of gels in panels A−D. Streptavidin displacement over time is shown in the presence of NS3 (1 μM) incubated with 10 nM 5′-bio-30-mer (circles), NS3 incubated with 10 nM 5′-bio-60-mer (diamonds), NS3 (100 nM) incubated with 200 nM 5′-bio-30-mer (squares), and NS3 (100 nM) incubated with 200 nM 5′-bio-60-mer (triangles).

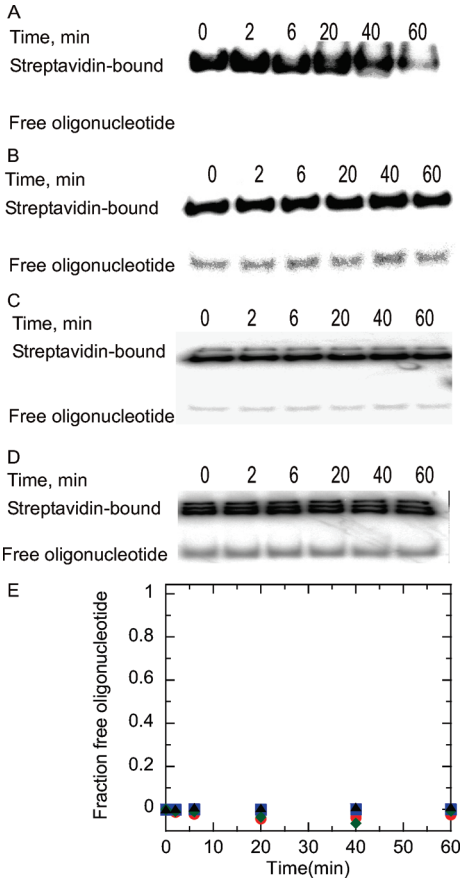

FIGURE 4: NS3h-catalyzed displacement of streptavidin from 5′-bio-30-mer and 5′-bio-60-mer oligonucleotides. (A) NS3h (1 μM) was incubated with 5′-bio-30-mer (10 nM) in reaction buffer (describe). Samples were removed at varying times and added to a quencher solution (0.6% SDS, 200 mM EDTA, 0.08% xylene cyanol, 0.08% bromophenol blue, and 10% glycerol) followed by separation of streptavidin-bound oligonucleotide from free oligonucleotide on a 15% native polyacrylamide gel. (B) NS3h (1 μM) was incubated with 10 nM 5′-bio-60-mer in reaction buffer and treated as described for panel A. (C) NS3h (100 nM) was incubated with 200 nM 5′-bio-30-mer under identical conditions as described for panel A, and samples were analyzed by 15% native polyacrylamide gel electrophoresis. (D) NS3h (100 nM) was incubated with 200 nM 5′-bio-60-mer under identical conditions as described for panel A. (E) Displacement of streptavidin from different lengths of biotin oligonucleotides catalyzed by NS3. Results were obtained by quantitation of gels in panels A−D. Streptavidin displacement over time is shown in the presence of NS3h (1 μM) incubated with 10 nM 5′-bio-30-mer (circles), NS3h incubated with 10 nM 5′-bio-60-mer (diamonds), NS3h (100 nM) incubated with 10 nM 5′-bio-30-mer (squares), and NS3h (100 nM) incubated with 10 nM 5′-bio-60-mer (triangles).

unwinding properties of these two helicases are similar when measured under identical conditions; however, their protein displacement activities are quite different.

We have added a new experiment in which NS3h dissociation was assessed on a biotin-labeled substrate in the presence or absence of streptavidin (Figure 6 of the Supporting Information). NS3h dissociates at a similar rate on each substrate. This indicates that when NS3h encounters streptavidin, it dissociates just as it would as if reaching the end of ssDNA. This result is in contrast to the result with Dda helicase, which was found to remain bound to ssDNA upon colliding with streptavidin (*45*). Previous results with other helicases indicated no difference between the BioTeg and Biotin dT linkers. In this paper, we used Biotin dT, and we mention this in Experimental Procedures. However, it is theoretically possible that different linkers might cause a difference. Examining the structural models of streptavidin bound to biotin-labeled DNA and considering the molecular structure of NS3h, we found it is difficult to imagine how NS3h might evade the streptavidin molecule during translocation.

NS3h Is a 3′−5′ Directionally Biased Single-Stranded DNA Translocase. The translocation of NS3 and NS3h along single-stranded DNA was monitored in a stopped-flow spectrometer using a previously established technique (*20*−*23*). This approach measures the change in fluorescence that occurs as a helicase translocates toward or away from a fluorescent label on ssDNA. The dependence of the observed time courses of fluorescence on the length of the oligonucleotide allows one to

determine the directionality and the kinetic parameters that govern translocation. We used a series of $(dT)_L$ molecules (L = 40−100 nucleotides) labeled at the 3′ or 5′ end with fluorescein [5′-F-$(dT)_L$ or 5′-$(dT)_L$-F] since the binding of enzyme to fluorescein results in a quenching of the fluorescence of the fluorophore (Figure 6). The protein trap heparin was also included in these reactions to ensure that any free enzyme in solution at the start of the reaction and any enzyme that dissociates during translocation will be unable to rebind the DNA and reinitiate translocation (*22*−*25*).

Multiple attempts to examine translocation of NS3 using different lengths of oligonucleotides labeled with fluorescein failed to produce interpretable data (Figure 2 of the Supporting Information). NS3 can exist as an oligomer containing multiple subunits. Preliminary experiments using DNA footprinting techniques indicate that NS3 binds along the entire length of the ssDNA due to protein−protein interactions (V. M. Raney and K. D. Raney, manuscript in preparation). This mode of binding precludes the study of translocation using the fluorescein-labeled substrates under conditions reported here, so alternative methods will be needed to examine translocation of this enzyme on ssDNA. Therefore, additional experiments were performed only with NS3h.

As shown in Figure 5A, when fluorescein is at the 3′ end of the ssDNA, only an increase in the fluorescence of the fluorophore is observed. Furthermore, the qualitative features of the time courses were independent of the length of the DNA. In contrast, when the fluorophore is at the 5′ end of the DNA, the observed time courses of fluorescence do depend upon the length of the DNA and are multiphasic; an initial rapid decrease in the fluorescence of the fluorophore is followed by a slow increase in fluorescence (Figure 5B). Taken together, these data support the conclusion that NS3h is a 3′−5′ directionally biased single-stranded DNA translocase (*14*).

Kinetic Analysis of NS3h Translocation along ssDNA Using Fluorescein-Labeled DNA. The fluorescence time courses resulting from stopped-flow experiments obtained with 5′-F-$(dT)_L$ (L = 40, 60, 72, 88, and 100) are shown in Figure 6. These experiments were conducted at 37 °C in assay buffer at a final heparin concentration of 4 mg/mL. The time courses of single-stranded DNA translocation by NS3h are qualitatively similar to those previously observed for single-stranded DNA translocation by the *E. coli* UvrD (*22*), *B. stearothermophilus* PcrA (*25*), and *E. coli* Rep (*26*) helicases, which suggests that a similar model for single-stranded DNA translocation may be applicable. It is worth noting, however, that there is evidence of a very fast initial phase in the time courses of single-stranded DNA translocation by NS3h occurring on a time scale faster than the first 50 ms of the reaction. The magnitude and duration of this fast phase, associated with a rapid increase in the fluorescence of the fluorophore, were independent of the length of the DNA, suggesting that it corresponds to a physical process conducted by proteins already bound close to the fluorophore before the addition of ATP. However, since the measurements of fluorophore fluorescence associated with these early time scales had large uncertainty, we did not attempt to model this phase directly. This omission will not affect our subsequent estimates of the kinetic parameters associated with the translocation of NS3h along single-stranded DNA since, as stated, the magnitude and duration of this phase were not dependent on the length of the single-stranded DNA.

The model for the mechanism of single-stranded DNA translocation by NS3h is shown in Scheme 1. In this model, an NS3h

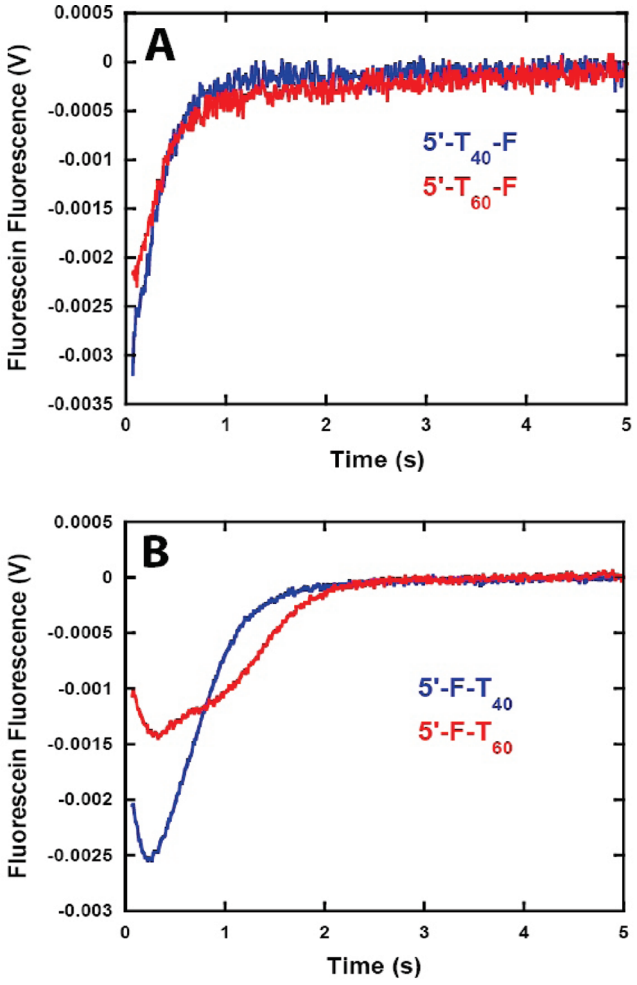

FIGURE 5: NS3h translocation kinetics monitored by stopped-flow experiments with fluorescein-labeled ssDNA. NS3h (100 nM) was preincubated with 200 nM ssDNA in assay buffer, and translocation was initiated by the addition of ATP (5 mM), $MgCl_2$ (10 mM), and heparin (4 mg/mL). (A) Fluorescence time courses obtained with 5′-$(dT)_{40}$-F (blue) and 5′-$(dT)_{60}$-F (red). (B) Fluorescence time courses obtained with 5′-F-$(dT)_{40}$ (blue) and 5′-F-$(dT)_{60}$ (red).

monomer with an occluded site size of b nucleotides and a contact size of d nucleotides binds with polarity to a single-stranded DNA that is L nucleotides long. The contact size, d, represents the number of consecutive nucleotides required to maintain all contacts with the protein and is less than or equal to the occluded site size of the protein. In this model, we assume that the protein utilizes its full contact size even when bound to the ends of the DNA (i.e., no dangling protein) (*22*). The NS3h monomer is initially bound i translocation steps from the 5′ end, with a concentration I_i. The number of translocation steps, i, is constrained ($1 \leq i \leq n$), where n is the maximum number of translocation steps needed for a translocase bound initially at the 3′ end to move to the 5′ end of a DNA that is L nucleotides long. We assume that the binding of NS3h to the single-stranded DNA is random, but uniform, so that there is an equal probability of binding to any position along the single-stranded DNA with the exception of the ends of the DNA, which have a different probability of binding.

Upon addition of ATP, the NS3h monomer moves with directional bias (from 3′ to 5′) along the DNA via a series of repeated rate-limiting translocation steps each associated with the same rate constant, k_t. The rate constant for protein dissociation

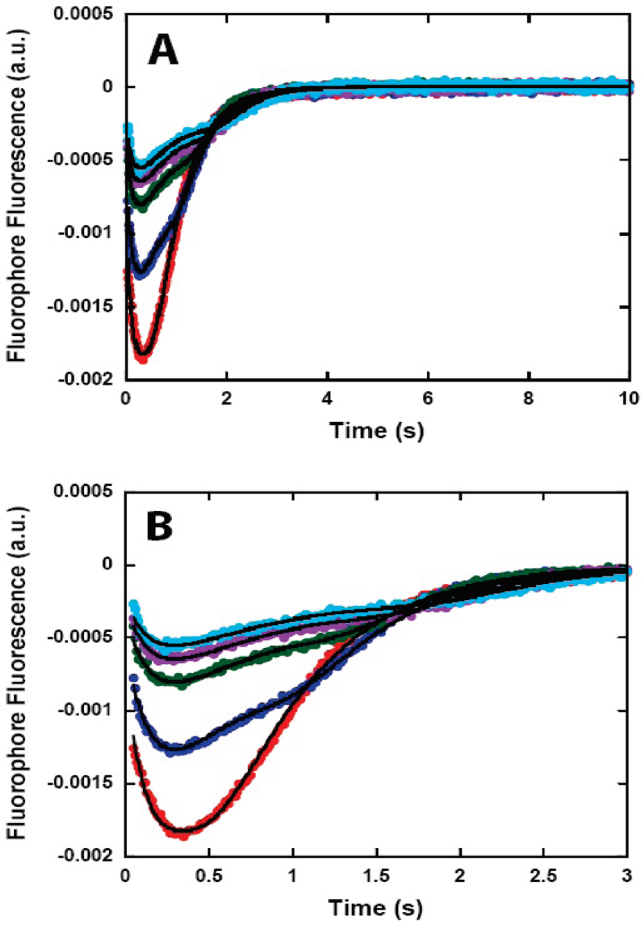

FIGURE 6: NS3h translocation kinetics monitored by stopped-flow experiments with fluorescein-labeled ssDNA. NS3h (100 nM) was pre-incubated with 200 nM ssDNA labeled at the 5′ end with fluorescein [5′-F-$(dT)_L$] at 37 °C in assay buffer, and translocation was initiated by the addition of ATP, Mg^{2+}, and heparin to final concentrations of 5 mM, 10 mM, and 4 mg/mL, respectively. Fluorescence time courses at short (A) and long (B) time scales obtained with 5′-F-$(dT)_{40}$ (red), 5′-F-$(dT)_{60}$ (blue), 5′-F-$(dT)_{72}$ (green), 5′-F-$(dT)_{88}$ (purple), and 5′-F-$(dT)_{100}$ (light blue). The solid lines are simulations using eq 1 and the best-fit parameters obtained from the global NLLS analysis of the time courses using eq 1.

during translocation is k_d. The finite processivity of translocation along the single-stranded DNA is thus defined as

$$P = \frac{k_t}{k_d + k_t}$$

Between each rate-limiting translocation step, the protein moves m nucleotides and the product mk_t is the macroscopic translocation rate and has units of nucleotides per second. Inclusion of a protein trap prevents any free protein that dissociates during translocation from rebinding to the DNA (*22*, *25*, *26*). When the protein reaches the 5′ end of the DNA (I_0 in Scheme 1) it dissociates from the DNA through a two-step process with associated rate constants k_c and k_{end}.

We note that, in general, k_t represents the rate constant for the rate-limiting step that occurs within each repeated translocation cycle and does not necessarily correspond to the rate constant for physical movement of the protein along the DNA (*22*). Similarly, the average number of nucleotides translocated between two successive rate-limiting steps, defined as the translocation "kinetic step size" (m), might be larger than the smallest length of DNA traversed during a single physical movement of the enzyme along the DNA.

On the basis of Scheme 1, the expressions in eq 1 can be derived (*22*, *25*) for the time-dependent accumulation of protein at the 5′ end of the DNA.

$$f(t) = L^{-1}\left[\left(A\left(1 + \frac{Bk_c}{s + k_{end}}\right)\left\{k_d + rk_t + s - \left(\frac{k_t}{k_d + k_t + s}\right)^n [rk_t + (r - rn)(k_d + s)]\right\}\right) \Big/ \{(k_c + s)(k_d + s)[1 + (n-1)r + rn]\}\right] \quad (1)$$

In these equations, L^{-1} is the inverse Laplace transform operator, s is the Laplace variable, and k_t, k_d, k_c, k_{end}, and n are as defined above. The variable A is a scalar factor incorporating both the initial concentration of protein bound to the single-stranded DNA and the fluorescence signal change associated with protein being bound at the 5′ end of the DNA (in the I_0 state in Scheme 1). The variable B is the ratio of the fluorescence signal change associated with a protein completing the second step of the two-step dissociation process to the fluorescence signal change associated with the protein being bound at the 5′ end of the DNA. The variable r is the ratio of the initial probability (before the addition of ATP) of the enzyme being bound to any other position (other than the 3′ or 5′ end) on the single-stranded DNA to the initial probability (before the addition of ATP) of the enzyme being bound to the 5′ end of the DNA (*22*). The variable rn is the ratio of the initial probability (before the addition of ATP) of the enzyme being bound to the 3′ end of the single-stranded DNA to the initial probability (before the addition of ATP) of the enzyme being bound to the 5′ end of the DNA. As shown in eq 2, we can relate n to the kinetic step size of translocation (m) and the interaction size of the enzyme on the DNA (d) (*21*, *22*, *25*, *26*).

$$n = \frac{L - d}{m} \quad (2)$$

Dissociation of NS3h from Internal Regions of ssDNA. Previous studies of the single-stranded DNA translocation activity of several bacterial helicases have relied upon independent measurements of the rate of dissociation from internal regions of the DNA (the k_d variable in Scheme 1 and eq 1) as a constraint in the NLLS analysis of the kinetic time courses (*22*, *25*, *26*, *46*). In an attempt to mimic this procedure, we monitored the dissociation kinetics of NS3h through changes in the intrinsic tryptophan fluorescence of the enzyme following its dissociation from poly(dT) and subsequent binding to heparin. NS3h (50 nM) was prebound to poly(dT) (5 μM nucleotide) in assay buffer, and dissociation was initiated by mixing with buffer containing 5 mM ATP, 10 mM $Mg(OAc)_2$, and various concentrations of heparin. The observed time courses (shown in Figure 7) are clearly biphasic and described well by simple two-exponential fits (eq 3). The results of linear least-squares fitting of the data in Figure 7 to eq 3 are listed in Table 1.

$$f(t) = A_0 + A_1 e^{-k_1 t} + A_2 e^{-k_2 t} \quad (3)$$

The analysis of these time courses indicates that no further changes in the kinetics of NS3h translocation, dissociation, and heparin binding occur beyond a heparin concentration of 2 mg/mL. This is consistent with our experimental results indicating that a heparin concentration of 2 mg/mL was sufficient to trap free

NS3h under these solution conditions (Figure 5 of the Supporting Information). However, the biphasic nature of all of the time courses in Figure 7 (including those obtained in the absence of heparin) and the observation that the associated rate constants ($k_{1,obs}$ and $k_{2,obs}$ in Table 1) decrease with an increase in heparin concentration make interpretation of the traces difficult. The second phase may represent photobleaching of NS3h over the time frame of the experiment. A control experiment was performed in the absence of ATP, and the decrease in fluorescence was similar to that observed in the presence of ATP (Figure 3 of the Supporting Information). The observation of a decrease in fluorescence in the absence of ATP indicates that the second phase is not likely related to translocation and may indeed be photobleaching. For this reason, we have analyzed the data in two ways. The value of k_d was allowed to float in the NLLS analysis, and the value was fixed according to the first observed rate constant obtained in Figure 7.

Mechanism of Single-Stranded DNA Translocation by NS3h. Estimates of the kinetic parameters in Scheme 1 were obtained through the global nonlinear least-squares analysis of the time courses in Figure 6 using eq 1. In this analysis, k_t, k_d, k_c, k_{end}, m, d, B, r, and rn were floated as global parameters (i.e., constrained to be the same for all single-stranded DNA lengths), whereas the A parameters were allowed to float independently for each single-stranded DNA length. The best-fit parameters obtained from global NLLS analysis of time courses in Figure 6 were as follows: $k_t = 28 \pm 4$ steps/s, $k_d = 0.2 \pm 0.06$ s^{-1}, $k_c = 6 \pm 1$ s^{-1}, $k_{end} = 1.8 \pm 0.1$ s^{-1}, and $m = 1.7 \pm 0.2$ nucleotides (summarized in Table 2). For comparison, rate constants obtained when the k_d value was fixed are reported in Table 2 of the Supporting Information. The macroscopic rate constant for translocation (mk_t) was determined to be 43 nucleotides/s when the value for k_d was allowed to float and 46 nucleotides/s when the value was fixed.

An equally probable representation of the kinetic mechanism for single-stranded DNA translocation by NS3h is shown in Scheme 2, and the associated equation for the fluorescence is eq 4.

$$f(t) = L^{-1}\left[(A/\{[1 + \mathrm{rn} + r(n-1)](k_i + s)\})\right.$$
$$\left.\left[C + (k_i\{k_d + rk_t + s - \left[k_t/(k_d + k_t + s)\right]^n[rk_t + (r - \mathrm{rn})(k_d + s)]\})/[(k_d + s)(k_{end} + s)]\right]\right] \quad (4)$$

In Scheme 2, the NS3h monomer is initially bound in a state that is not competent for processive DNA translocation (the I_i* concentrations in Scheme 2). The variable k_i in this scheme and eq 4 is the rate constant for the translocation initiation process that occurs after the binding of ATP; the variables k_t, k_d, k_{end}, m, d, r, and rn in Scheme 2 and eq 4 are as defined for Scheme 1 and eq 1. The variable C is the ratio of the fluorescence signal change associated with an enzyme bound at the 5′ end of the DNA in the preinitiation state (the I_o* concentration in Scheme 2) to the fluorescence signal change associated with an enzyme bound at the 5′ end in the postinitiation state (the I_0 concentration in Scheme 2). The best-fit parameters obtained from global NLLS analysis of time courses in Figure 6 according to Scheme 2 (eq 4) are as follows: $k_t = 30 \pm 6$ steps/s, $k_d = 0.2 \pm 0.06$ s^{-1}, $k_c = 6 \pm 1$ s^{-1}, $k_{end} = 1.8 \pm 0.1$ s^{-1}, and $m = 1.4 \pm 0.3$ nucleotides (summarized in Table 2). The fits of the data in Figure 6 using eq 4 overlay perfectly with the fits obtained using eq 1 (as indicated by the identical variance of the fit in Table 2).

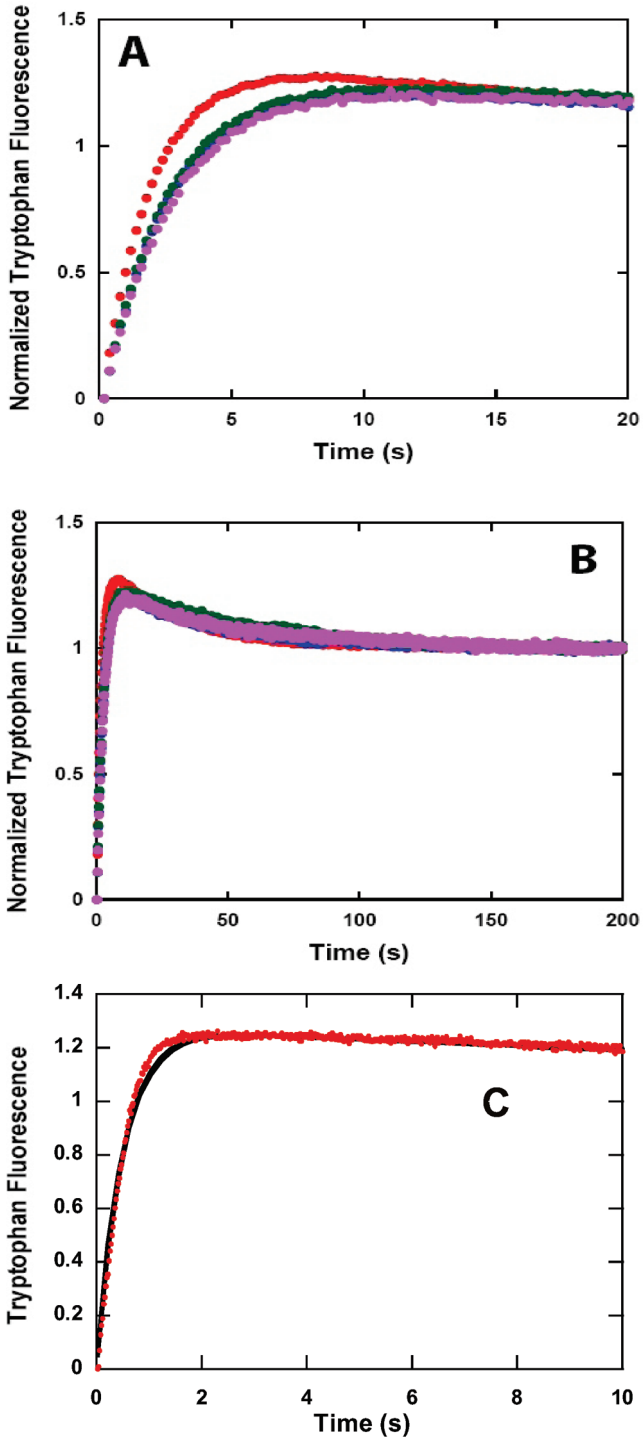

FIGURE 7: NS3h translocation along poly(dT) monitored by stopped-flow fluorescence spectroscopy of the intrinsic tryptophan fluorescence of NS3h for short (A) and long (B) time scales. NS3h (50 nM) was prebound to poly(dT) (5 μM nucleotide) in assay buffer, and translocation was initiated when the sample was mixed with buffer containing ATP (5 mM), $Mg(OAc)_2$ (10 mM), and various concentrations of heparin. Fluorescence time courses are shown with final heparin concentrations of 0 (red), 2 (blue), 4 (green), and 6 mg/mL (purple). (C) NS3h (100 nM) was prebound to a 37-mer·22-mer complex (200 nM) in assay buffer, and translocation was initiated when the sample was mixed with buffer containing ATP (5 mM), $Mg(OAc)_2$ (10 mM), and heparin (4 mg/mL). Fluorescence data were fit to the sum of two exponentials, resulting in rate constants of 2.0 ± 0.01 s^{-1} for the first exponential phase and 0.029 ± 0.006 s^{-1} for the second exponential phase of the progress curve.

Table 1: Linear Least-Squares Fitting of the Data in Figure 7

[heparin] (mg/mL)	$k_{1,obs}$ (s^{-1})	$k_{2,obs}$ (s^{-1})
0	0.54 ± 0.04	0.038 ± 0.003
2	0.41 ± 0.05	0.026 ± 0.004
4	0.42 ± 0.03	0.018 ± 0.002
6	0.40 ± 0.04	0.022 ± 0.003

Table 2: Best-Fit Parameters Obtained from Global NLLS Analysis of the Data in Figure 6

Scheme 1		Scheme 2	
k_t (steps/s)	27 ± 3	k_t (steps/s)	30 ± 6
k_d (s^{-1})	0.2 ± 0.06	k_d (s^{-1})	0.20 ± 0.06
k_c (s^{-1})	6 ± 1	k_i (s^{-1})	6 ± 1
k_{end} (s^{-1})	1.8 ± 0.1	k_{end} (s^{-1})	1.8 ± 0.1
m (nucleotides/step)	1.7 ± 0.2	m (nucleotides/step)	1.4 ± 0.3
d (nucleotides)	21 ± 4	d (nucleotides)	19 ± 4
r	0.028 ± 0.004	r	0.024 ± 0.005
rn	0.22 ± 0.05	rn	0.19 ± 0.04
B	8.3 ± 1.3	C	0.30 ± 0.08
mk_t (nucleotides/s)	46 ± 5	mk_t (nucleotides/s)	46 ± 5
$m/(1 - P)$ (nucleotides)	230 ± 60	$m/(1 - P)$ (nucleotides)	230 ± 80
variance	4.39×10^{-10}	variance	4.39×10^{-10}

It is worth noting that correlation exists between some sets of parameters in these equations; the parameters k_t, m, r, and rn are especially highly correlated with each other, for example. Therefore, coupled variations in these parameters can result in nearly equally good fits of the data (see Table 1 of the Supporting Information). We would like to emphasize, however, that the estimate of the macroscopic translocation rate (mk_t) is well-constrained by the data, regardless of variations in k_t or m. As shown in the Supporting Information, although reasonable fits of the time courses, as judged by their variances, are obtained when k_t is constrained to values in the range from 27 to 270 steps/s, the estimate of the macroscopic translocation rate remains similar. Similarly, when the k_d value for dissociation of NS3h from poly(dT) is fixed on the basis of the rate of the first exponential from data in Figure 7, the macroscopic rate constant for translocation remains similar to that obtained when the k_d value is allowed to float (Table 2 of the Supporting Information). Taken together, we believe that the macroscopic translocation rate is more accurately constrained by our analysis than the associated microscopic translocation rate. Similarly, we believe that the estimate of the macroscopic translocation rate is more accurately constrained than the estimates of binding parameters r and rn.

Translocation experiments were conducted with Cy3-labeled oligonucleotides to compare results obtained with fluorescein-labeled oligonucleotides (Figure 4 of the Supporting Information). The estimate of d is larger for the Cy3 substrates, and the estimate of mk_t is smaller for the Cy3 substrates (Table 3 of the Supporting Information). Similar trends in the variation of the estimates of d and mk_t between F- and Cy3-labeled DNA were observed previously in the case of UvrD and were attributed to a difference in the physical distances over which UvrD could interact with these fluorophores and subsequently affect their fluorescence (*20*). Our results suggest that a similar difference in interaction distance between NS3h and these same fluorophores also occurs.

Dissociation of NS3h from DNA Unwinding Substrate. The lack of product formation during unwinding by monomeric NS3h under single-cycle conditions is surprising in light of the relatively fast rate of translocation on ssDNA (~46 nucleotides/s). The unwinding rate measured in the presence of an excess concentration of NS3h relative to DNA was 0.61 s^{-1} for the 22 bp substrate (Figure 1). The final 8−10 bp melt spontaneously (*38*), so we can assume that ~12 bp are melted by the action of the helicase, leading to a rate for unwinding of 7.3 bp/s. The movement of NS3h along DNA clearly slows when NS3h encounters duplex DNA.

The rate of dissociation of NS3h from the ssDNA−dsDNA substrate was measured by using stopped-flow fluorescence spectroscopy under conditions that were identical to those used for measuring translocation. NS3h (100 nM) was incubated with the 37-mer·22-mer complex (200 nM) followed by rapid mixing with ATP, Mg^{2+}, and heparin, resulting in a dissociation rate constant of 2.0 ± 0.01 s^{-1} (Figure 7C). This dissociation rate constant is ~5-fold faster than rate of dissociation from ssDNA (compare to Figure 7A). Therefore, when NS3h encounters duplex DNA, it dissociates faster than when translocating on ssDNA. The combination of slower movement through the duplex and faster dissociation leads to relatively poor DNA unwinding activity by NS3h when compared to its translocase activity.

DISCUSSION

The mechanism of processive DNA unwinding by helicases has been linked to the mechanism of translocation on ssDNA (*16*, *22*). Mechanisms in which melting of a base pair occurs, followed by translocation of one nucleotide in a process that is coupled to ATP binding and hydrolysis, have been proposed. The steps for melting the dsDNA and translocation on ssDNA have been proposed to be separable in some cases (*43*). For other helicases such as Dda, dsDNA unwinding has been proposed to be a consequence of translocation on ssDNA (*13*, *17*), whereby movement of the enzyme along the DNA forces apart the base pairs. It is clear, however, that some helicases can readily translocate on ssDNA yet are unable to unwind duplexes under single-cycle conditions (*21*, *25*). Hence, the ability to translocate on ssDNA is not necessarily sufficient for DNA unwinding.

Protein displacement has been suggested as an important biological role played by helicases. During homologous recombination in *Saccharomyces cerevisiae*, Rad51 protein serves as a recombinase by forming filaments on ssDNA (*47*, *48*). Srs2 is a superfamily 1 helicase that disassembles Rad51 nucleoprotein filaments, thereby suppressing homologous recombination (*49*, *50*). The physical interaction between Srs2 and Rad51 triggers ATP hydrolysis within the Rad51 filament, causing Rad51 to dissociate from DNA (*51*). However, an ATPase-deficient form of Srs2 was unable to stimulate disassembly of Rad51 filaments, indicating that translocase activity of Srs2 also plays a role in the removal of the protein filament. Understanding the relationships among translocation, DNA unwinding, and protein displacement is necessary to define the biochemical activities of many helicases.

NS3 (and/or the NS3 helicase domain) from the hepatitis C virus has become one of the most studied SF2 helicases. In addition to its medical importance related to viral infection and liver disease, NS3 is considered a model system for this group of enzymes. Translocation and melting have been proposed to be linked but occur in separate steps in a spring-loaded mechanism, based on stepping measurements made using single-molecule FRET to study DNA unwinding (*36*). Here we have investigated

the relationship among translocation, DNA unwinding, and protein displacement by examining each reaction under identical conditions.

Full-length NS3 contains a helicase domain and a protease domain which can be expressed and studied separately. Each form of the enzyme was studied under identical conditions in this report. Little or no unwinding is observed for each form of the enzyme when the DNA substrate concentration is in excess of the enzyme concentration under single-cycle conditions (Figure 2). The lack of product does not mean that the monomeric enzyme does not unwind DNA. When one molecule of enzyme binds to the DNA substrate, the helicase dissociates prior to unwinding a sufficient portion of the 22 bp substrate to observe ssDNA under single-cycle conditions. Under identical conditions (substrate concentration greater than enzyme concentration), NS3h clearly translocates on ssDNA (Figure 6). The number of nucleotides translocated in a single binding event is around 230. The fact that only 22 bp are not unwound in a single cycle indicates that unwinding of dsDNA alters the activity of NS3h significantly. The rate of DNA unwinding by NS3h is reduced compared to the rate of translocation on ssDNA. The rate of dissociation of NS3h from the duplex substrate was 5-fold faster than the rate of dissociation from ssDNA. DNA unwinding by NS3h has been shown to be sensitive to the stability of the base pairs within the duplex (*52*). Movement of the enzyme is therefore impeded by duplex DNA, and the results here are consistent with this interpretation.

Under conditions in which the enzyme concentration exceeds the DNA substrate concentration, NS3h unwinds the 22 bp substrate (Figure 1). Multiple molecules of NS3h bound to the same DNA substrate molecule can increase the amount of product for DNA unwinding through functional cooperativity (*38*). Single-stranded DNA binding proteins can also function with NS3h to increase DNA unwinding activity, possibly by interacting directly with the helicase and by preventing reannealing of the DNA after helicase-catalyzed unwinding (*39*). NS3h clearly requires other molecules for optimal DNA unwinding activity. The reason for this requirement may relate to the affinity of NS3h for DNA during the ATP hydrolysis cycle. A "weak state" of interaction has been reported for the ATP-bound form of NS3h (*53*). SSB or additional helicase molecules may serve as processivity factors that hold NS3h onto the DNA during the weak binding state of the cycle, thereby enhancing the opportunity for overcoming the barrier presented by dsDNA.

Determining the relationship between ssDNA translocation and DNA unwinding by NS3h is made difficult by the fact that NS3h does not readily unwind DNA under the conditions in which translocation can be measured. If NS3h-catalyzed DNA unwinding were observed under these conditions, then kinetic parameters from the two methods could be directly compared with confidence. However, the kinetic parameters for translocation can be compared to kinetic parameters for DNA unwinding obtained from experiments under excess enzyme conditions. The kinetic step size obtained for translocation of NS3h on ssDNA was 1.4−1.7 bp/step (Table 2). We note that this microscopic parameter is less well-constrained than macroscopic parameters such as the rate of translocation. However, it is worth discussing this value in the context of measurements of step size provided by other laboratories.

Such a relatively small kinetic step size implies that the physical step size for NS3h is likely to be 1 or 2 bp (*34*). Larger kinetic step sizes have been reported for DNA and RNA unwinding. A kinetic step size of 9 bp was measured for NS3h under excess enzyme conditions (*38*). RNA unwinding studies resulted in a kinetic step size of ~18 bp for full-length NS3 (*33*). The larger kinetic step sizes are likely made up of smaller, substeps. Single-molecule approaches have provided measurements of the physical step size for full-length NS3 of 11 bp for RNA unwinding with smaller substeps of 2−3 bp (*35*). Single-molecule FRET experiments were interpreted in terms of a physical step size of ~3 bp, which was made up of smaller 1 bp substeps (*36*). The smaller steps measured by single-molecule measurements indicate that one ATP hydrolysis event per NS3 molecule is likely to lead to movement by 1 bp.

Most recently, Serebrov et al. demonstrated that kinetic step size (16 bp/step) was independent of RNA duplex stability and composition but is dependent on salt concentration (*54*). Unwinding was enhanced under low-salt conditions by monomeric NS3, and step size was decreased to 11 bp/step. The "supersteps" (11 and 18 bp) observed in RNA unwinding were thought to be caused by delayed product release of separated RNA product from domain II of NS3 (*54*). The kinetic step size of NS3h, 1.4−1.7 nucleotides, reported here under monomeric conditions can be readily interpreted to indicate a movement of 1 or 2 bp per ATP binding and hydrolysis event, which is consistent with the results from single-molecule FRET studies. The fact that DNA unwinding is not occurring during the translocation assays means that product release of the displaced strand is not part of the mechanism and may explain the lack of supersteps observed in the translocase assay. Direct measurements of ATPase activity are needed to further test the idea that NS3h moves by one base per ATP hydrolysis event (*16*, *21*, *23*).

Attempts to examine translocation using fluorescently labeled oligonucleotides did not succeed for full-length NS3 (Figure 1 of the Supporting Information). The lack of clearly defined changes in fluorescence as a function of oligonucleotide length for NS3 might be a result of the oligomeric nature of the enzyme under these conditions. For example, oligomeric NS3 might exist in a form that binds to multiple sites along the single-stranded DNA, essentially coating the DNA. This would lead to the fluorescent probe being bound by NS3 at the start of the reaction, regardless of the length of the oligonucleotide. Much longer oligonucleotides might be needed to measure the translocase activity of oligomeric NS3, or an alternative method needs to be developed that examines each individual binding site along the DNA. ATPase activity has been measured as a function of ssDNA length for several helicases to infer translocation mechanisms, and such methods may apply for full-length NS3 (*23*).

Displacement of streptavidin is observed for NS3, but not for NS3h, and only when the NS3 concentration is in excess of the substrate concentration (Figures 3 and 4). Others have reported streptavidin displacement by NS3h (*55*); however, we were unable to observe this activity under conditions described here. The lack of displacement by NS3h is surprising, especially in light of the demonstrable translocase activity. This result illustrates that translocation per se does not provide sufficient force to dislodge streptavidin from the biotin-labeled oligonucleotides, at least under the conditions examined here. Force production might require specific interactions between helicase and DNA that are not present in NS3h. The X-ray crystal structure of NS3h bound to DNA indicates that the majority of interactions are electrostatic in nature, although some stacking interactions between the nucleobase and amino acids are also observed (*40*). Full-length NS3 binds more tightly to DNA than NS3h, which

might allow greater force production during translocation due to additional contacts made with nucleic acid through the protease domain of NS3 (*32*, *54*).

Interestingly, our results also suggest a preference for NS3h to bind to the ends of the single-stranded DNA, rather than to the middle ($r \ll 1$ in Table 1). This is in contrast to what has been observed with several bacterial helicases (UvrD, PcrA, and Rep) and warrants further investigation. This preference for binding to the ends of the single-stranded DNA may also be responsible for the apparent inflation of the estimate of the interaction size of NS3h on the single-stranded DNA ($d \sim 20$ nucleotides in Table 1).

The experiments reported here indicate that NS3h translocates 46 ± 5 nucleotides/s with a step size of $1.4-1.7 \pm 0.5$ nucleotides/step and a processivity of 230 ± 60 nucleotides. From these results, one can predict that NS3h should unwind short duplex DNA and displace proteins bound to DNA (streptavidin) under identical conditions. Interestingly, NS3h was unable to unwind the 22 bp duplex substrate and could not displace streptavidin from biotin-labeled DNA under the conditions in which translocation was measured. Therefore, optimal DNA unwinding and protein displacement by NS3h require more than simply translocation. Interaction with other proteins such as single-stranded binding proteins (*39*) or function with additional molecules of NS3h (*38*) can result in enhanced helicase activity for this ssDNA translocase.

SUPPORTING INFORMATION AVAILABLE

Data on size exclusion chromatography of NS3h in the presence of ssDNA, NS3 translocation on 5′-F-$(dT)_L$, NS3 translocation on poly(dT)/M13, NS3h translocation on Cy3-labeled oligos, NS3h translocation in the presence of different concentrations of heparin, and NS3h translocation on biotinylated oligo (3′-T58-bio-dTG-5′) in the presence and absence of streptavidin. This material is available free of charge via the Internet at http://pubs.acs.org.

REFERENCES

1. Singleton, M. R., Dillingham, M. S., and Wigley, D. B. (2007) Structure and mechanism of helicases and nucleic acid translocases. *Annu. Rev. Biochem. 76*, 23–50.
2. Lohman, T. M., Tomko, E. J., and Wu, C. G. (2008) Non-hexameric DNA helicases and translocases: Mechanisms and regulation. *Nat. Rev. Mol. Cell Biol. 9*, 391–401.
3. Patel, S. S., and Donmez, I. (2006) Mechanisms of helicases. *J. Biol. Chem. 281*, 18265–18268.
4. Pyle, A. M. (2008) Translocation and unwinding mechanisms of RNA and DNA helicases. *Annu. Rev. Biophys. 37*, 317–336.
5. Gorbalenya, A. E., and Koonin, E. V (1993) Helicases: Amino acid sequence comparisons and structure-function relationships. *Curr. Opin. Struct. Biol. 3*, 419–429.
6. Maluf, N. K., Fischer, C. J., and Lohman, T. M. (2003) A Dimer of *Escherichia coli* UvrD is the active form of the helicase in vitro. *J. Mol. Biol. 325*, 913–935.
7. Nanduri, B., Byrd, A. K., Eoff, R. L., Tackett, A. J., and Raney, K. D. (2002) Pre-steady-state DNA unwinding by bacteriophage T4 Dda helicase reveals a monomeric molecular motor. *Proc. Natl. Acad. Sci. U.S.A. 99*, 14722–14727.
8. Patel, S. S., and Picha, K. M. (2000) Structure and function of hexameric helicases. *Annu. Rev. Biochem. 69*, 651–697.
9. Singleton, M. R., Dillingham, M. S., Gaudier, M., Kowalczykowski, S. C., and Wigley, D. B. (2004) Crystal structure of RecBCD enzyme reveals a machine for processing DNA breaks. *Nature 432*, 187–193.
10. Velankar, S. S., Soultanas, P., Dillingham, M. S., Subramanya, H. S., and Wigley, D. B. (1999) Crystal structures of complexes of PcrA DNA helicase with a DNA substrate indicate an inchworm mechanism. *Cell 97*, 75–84.
11. Eggleston, A. K., O'Neill, T. E., Bradbury, E. M., and Kowalczykowski, S. C. (1995) Unwinding of nucleosomal DNA by a DNA helicase. *J. Biol. Chem. 270*, 2024–2031.
12. Byrd, A. K., and Raney, K. D. (2004) Protein displacement by an assembly of helicase molecules aligned along single-stranded DNA. *Nat. Struct. Mol. Biol. 11*, 531–538.
13. Morris, P. D., and Raney, K. D. (1999) DNA helicases displace streptavidin from biotin-labeled oligonucleotides. *Biochemistry 38*, 5164–5171.
14. Morris, P. D., Byrd, A. K., Tackett, A. J., Cameron, C. E., Tanega, P., Ott, R., Fanning, E., and Raney, K. D. (2002) Hepatitis C virus NS3 and simian virus 40 T antigen helicases displace streptavidin from 5′-biotinylated oligonucleotides but not from 3′-biotinylated oligonucleotides: Evidence for directional bias in translocation on single-stranded DNA. *Biochemistry 41*, 2372–2378.
15. van Brabant, A. J., Stan, R., and Ellis, N. A. (2000) DNA helicases, genomic instability, and human genetic disease. *Annu. Rev. Genomics Hum. Genet. 1*, 409–459.
16. Dillingham, M. S., Wigley, D. B., and Webb, M. R. (2000) Demonstration of unidirectional single-stranded DNA translocation by PcrA helicase: Measurement of step size and translocation speed. *Biochemistry 39*, 205–212.
17. Tackett, A. J., Morris, P. D., Dennis, G. E., and Raney, K. D. (2001) Unwinding of unnatural substrates by a DNA helicase. *Biochemistry 40*, 543–548.
18. Walstrom, K. M., Dozono, J. M., Robic, S., and von Hippel, P. H. (1997) Kinetics of the RNA-DNA Helicase Activity of *Escherichia coli* Transcription Termination Factor Rho. 1. Characterization and Analysis of the Reaction. *Biochemistry 36*, 7980–7992.
19. Walstrom, K. M., Dozono, J. M., and von Hippel, P. H. (1997) Kinetics of the RNA-DNA Helicase Activity of *Escherichia coli* Transcription Termination Factor Rho. 2. Processivity, ATP Consumption, and RNA Binding. *Biochemistry 36*, 7993–8004.
20. Soultanas, P., Dillingham, M. S., Wiley, P., Webb, M. R., and Wigley, D. B. (2000) Uncoupling DNA translocation and helicase activity in PcrA: Direct evidence for an active mechanism. *EMBO J. 19*, 3799–3810.
21. Dillingham, M. S., Wigley, D. B., and Webb, M. R. (2002) Direct measurement of single-stranded DNA translocation by PcrA helicase using the fluorescent base analogue 2-aminopurine. *Biochemistry 41*, 643–651.
22. Fischer, C. J., Maluf, N. K., and Lohman, T. M. (2004) Mechanism of ATP-dependent translocation of *E. coli* UvrD monomers along single-stranded DNA. *J. Mol. Biol. 344*, 1287–1309.
23. Tomko, E. J., Fischer, C. J., Niedziela-Majka, A., and Lohman, T. M. (2007) A nonuniform stepping mechanism for *E. coli* UvrD monomer translocation along single-stranded DNA. *Mol. Cell 26*, 335–347.
24. Maluf, N. K., Ali, J. A., and Lohman, T. M. (2003) Kinetic mechanism for formation of the active, dimeric UvrD helicase-DNA complex. *J. Biol. Chem. 278*, 31930–31940.
25. Niedziela-Majka, A., Chesnik, M. A., Tomko, E. J., and Lohman, T. M. (2007) *Bacillus stearothermophilus* PcrA monomer is a single-stranded DNA translocase but not a processive helicase in vitro. *J. Biol. Chem. 282*, 27076–27085.
26. Brendza, K. M., Cheng, W., Fischer, C. J., Chesnik, M. A., Niedziela-Majka, A., and Lohman, T. M. (2005) Autoinhibition of *Escherichia coli* Rep monomer helicase activity by its 2B subdomain. *Proc. Natl. Acad. Sci. U.S.A. 102*, 10076–10081.
27. Anand, S. P., Zheng, H., Bianco, P. R., Leuba, S. H., and Khan, S. A. (2007) DNA helicase activity of PcrA is not required for the displacement of RecA protein from DNA or inhibition of RecA-mediated strand exchange. *J. Bacteriol. 189*, 4502–4509.
28. Veaute, X., Delmas, S., Selva, M., Jeusset, J., Cam, E. L., Matic, I., Fabre, F., and Petit, M.-A. (2005) UvrD helicase, unlike Rep helicase, dismantles RecA nucleoprotein filaments in *Escherichia coli*. *EMBO J. 24*, 180–189.
29. Tai, C. L., Chi, W. K., Chen, D. S., and Hwang, L. H. (1996) The helicase activity associated with hepatitis C virus nonstructural protein 3 (NS3). *J. Virol. 70*, 8477–8484.
30. Kim, D. W., Gwack, Y., Han, J. H., and Choe, J. (1995) C-terminal domain of the hepatitis C virus NS3 protein contains an RNA helicase activity. *Biochem. Biophys. Res. Commun. 215*, 160–166.
31. Tackett, A. J., Chen, Y., Cameron, C. E., and Raney, K. D. (2005) Multiple full-length NS3 molecules are required for optimal unwinding of oligonucleotide DNA in vitro. *J. Biol. Chem. 280*, 10797–10806.
32. Sikora, B., Chen, Y., Lichti, C. F., Harrison, M. K., Jennings, T. A., Tang, Y., Tackett, A. J., Jordan, J. B., Sakon, J., Cameron, C. E., and Raney, K. D. (2008) Hepatitis C virus NS3 helicase forms oligomeric

structures that exhibit optimal DNA unwinding activity in vitro. *J. Biol. Chem. 283*, 11516–11525.
33. Serebrov, V., and Pyle, A. M. (2004) Periodic cycles of RNA unwinding and pausing by hepatitis C virus NS3 helicase. *Nature 430*, 476–480.
34. Galletto, R., Jezewska, M. J., and Bujalowski, W. (2004) Unzipping mechanism of the double-stranded DNA unwinding by a hexameric helicase: Quantitative analysis of the rate of the dsDNA unwinding, processivity and kinetic step size of the *Escherichia coli* DnaB helicase using rapid quench-flow method. *J. Mol. Biol. 343*, 83–99.
35. Dumont, S., Cheng, W., Serebrov, V., Beran, R. K., Tinoco, I., Jr., Pyle, A. M., and Bustamante, C. (2006) RNA translocation and unwinding mechanism of HCV NS3 helicase and its coordination by ATP. *Nature 439*, 105–108.
36. Myong, S., Bruno, M. M., Pyle, A. M., and Ha, T. (2007) Spring-loaded mechanism of DNA unwinding by hepatitis C virus NS3 helicase. *Science 317*, 513–516.
37. Levin, M. K., Gurjar, M., and Patel, S. S. (2005) A Brownian motor mechanism of translocation and strand separation by hepatitis C virus helicase. *Nat. Struct. Mol. Biol. 12*, 429–435.
38. Levin, M. K., Wang, Y. H., and Patel, S. S. (2004) The functional interaction of the hepatitis C virus helicase molecules is responsible for unwinding processivity. *J. Biol. Chem. 279*, 26005–26012.
39. Rajagopal, V., and Patel, S. S. (2008) Single strand binding proteins increase the processivity of DNA unwinding by the hepatitis C virus helicase. *J. Mol. Biol. 376*, 69–79.
40. Mackintosh, S. G., Lu, J. Z., Jordan, J. B., Harrison, M. K., Sikora, B., Sharma, S. D., Cameron, C. E., Raney, K. D., and Sakon, J. (2006) Structural and biological identification of residues on the surface of NS3 helicase required for optimal replication of the hepatitis C virus. *J. Biol. Chem. 281*, 3528–3535.
41. Williams, D. J., and Hall, K. B. (2000) Monte Carlo application to thermal and chemical denaturation experiments of nucleic acids and proteins. *Methods Enzymol. 321*, 330–352.
42. Porter, D. J., and Preugschat, F. (2000) Strand-separating activity of hepatitis C virus helicase in the absence of ATP. *Biochemistry 39*, 5166–5173.
43. Pang, P. S., Jankowsky, E., Planet, P. J., and Pyle, A. M. (2002) The hepatitis C viral NS3 protein is a processive DNA helicase with cofactor enhanced RNA unwinding. *EMBO J. 21*, 1168–1176.
44. Porter, D. J. T., Short, S. A., Hanlon, M. H., Preugschat, F., Wilson, J. E., Willard, D. H., Jr., and Consler, T. G. (1998) Product Release Is the Major Contributor to k_{cat} for the Hepatitis C Virus Helicase-catalyzed Strand Separation of Short Duplex DNA. *J. Biol. Chem. 273*, 18906–18914.
45. Raney, K. D., and Benkovic, S. J. (1995) Bacteriophage T4 Dda helicase translocates in a unidirectional fashion on single-stranded DNA. *J. Biol. Chem. 270*, 22236–22242.
46. Fischer, C. J., and Lohman, T. M. (2004) ATP-dependent translocation of proteins along single-stranded DNA: Models and methods of analysis of pre-steady state kinetics. *J. Mol. Biol. 344*, 1265–1286.
47. Zaitseva, E. M., Zaitsev, E. N., and Kowalczykowski, S. C. (1999) The DNA binding properties of *Saccharomyces cerevisiae* Rad51 protein. *J. Biol. Chem. 274*, 2907–2915.
48. Bianco, P. R., Tracy, R. B., and Kowalczykowski, S. C. (1998) DNA strand exchange proteins: A biochemical and physical comparison. *Front. Biosci. 3*, D570–D603.
49. Krejci, L., Van Komen, S., Li, Y., Villemain, J., Reddy, M. S., Klein, H., Ellenberger, T., and Sung, P. (2003) DNA helicase Srs2 disrupts the Rad51 presynaptic filament. *Nature 423*, 305–309.
50. Veaute, X., Jeusset, J., Soustelle, C., Kowalczykowski, S. C., Le Cam, E., and Fabre, F. (2003) The Srs2 helicase prevents recombination by disrupting Rad51 nucleoprotein filaments. *Nature 423*, 309–312.
51. Antony, E., Tomko, E. J., Xiao, Q., Krejci, L., Lohman, T. M., and Ellenberger, T. (2009) Srs2 Disassembles Rad51 Filaments by a Protein-Protein Interaction Triggering ATP Turnover and Dissociation of Rad51 from DNA. *Mol. Cell 35*, 105–115.
52. Donmez, I., Rajagopal, V., Jeong, Y.-J., and Patel, S. (2007) Nucleic acid unwinding by hepatitis C virus and bacteriophage T7 helicases is sensitive to base pair stability. *J. Biol. Chem. 282*, 21116–21123.
53. Levin, M. K., Gurjar, M., and Patel, S. S. (2003) ATP binding modulates the nucleic acid affinity of hepatitis C virus helicase. *J. Biol. Chem. 278*, 23311–23316.
54. Serebrov, V., Beran, R. K., and Pyle, A. M. (2008) Establishing a mechanistic basis for the large kinetic steps of the NS3 helicase. *J. Biol. Chem. 284*, 2512–22521.
55. Lam, A. M., Keeney, D., and Frick, D. N. (2003) Two novel conserved motifs in the hepatitis C virus NS3 protein critical for helicase action. *J. Biol. Chem. 278*, 44514–44524.